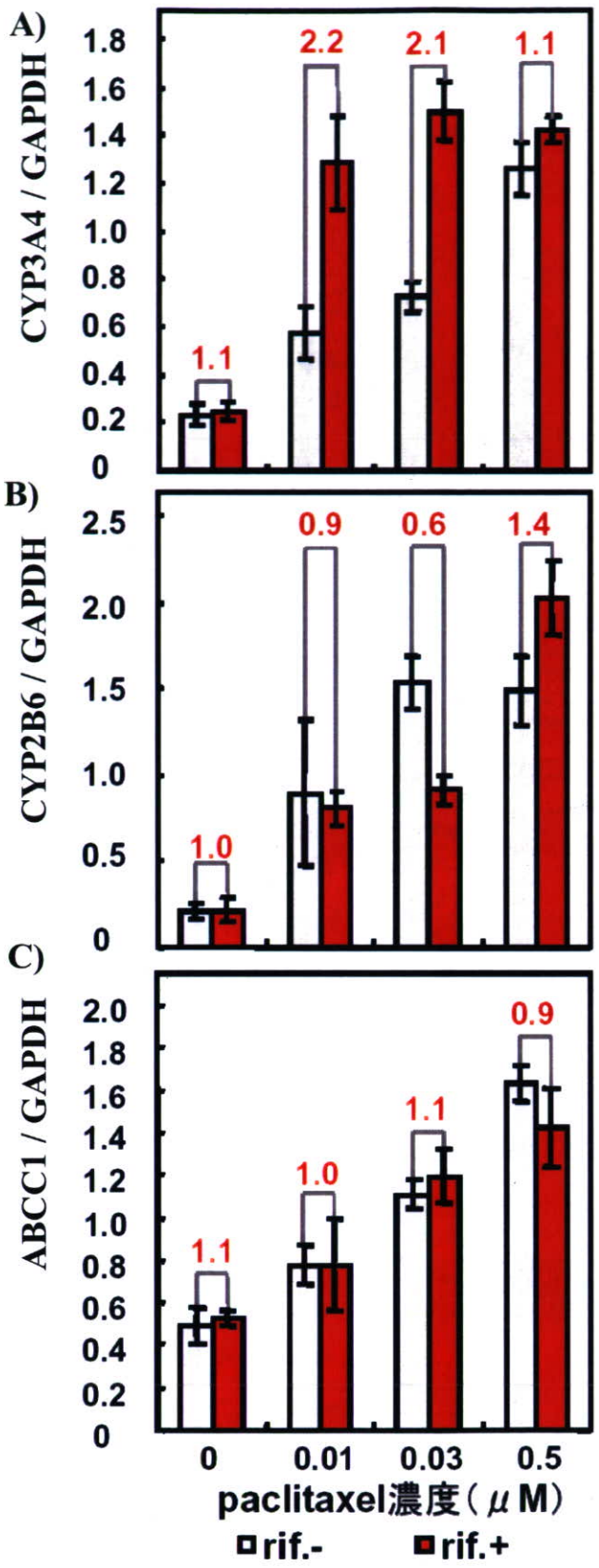


**Fig. 31 paclitaxel処理のrifampicinによる誘導への影響**

Paclitaxel処理（0μM、0.01μM、0.03μM,0.5μM）を行った際に、rifampicn処理を行った場合と行わなかった場合の*CYP3A4*、*CYP2B6*、*ABCC1*の発現量を示した。各遺伝子の発現量はRT-PCRで得られた相対発現量をGAPDHの相対発現量で正規化した値である。

A) *CYP3A4*　B) *CYP2B6*　C) *ABCC1*

参考．microRNA (miRNA)、*CYP3A4*の構造、miRNAの検索結果

**参Fig. 1. Processing pathway of miRNA**

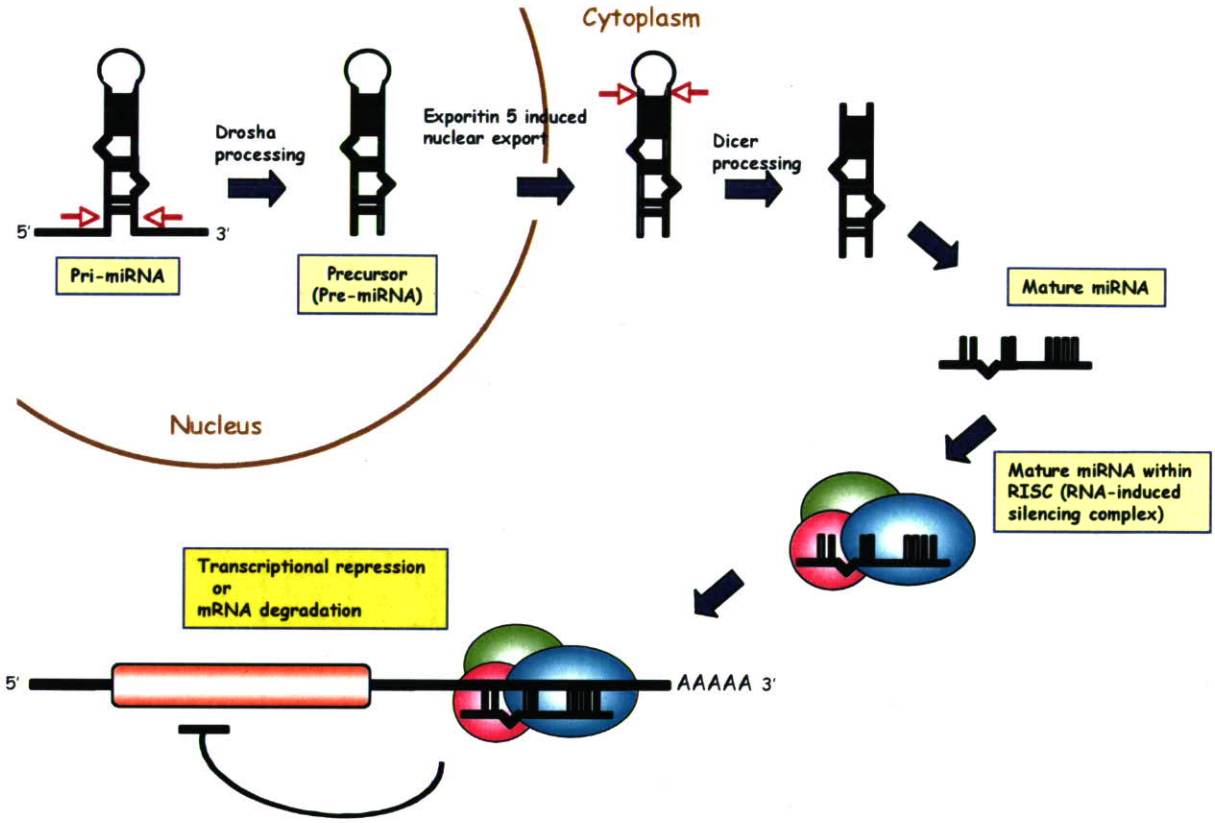


**参Fig. 2. *CYP3A* genes cluster in Chr. 7**

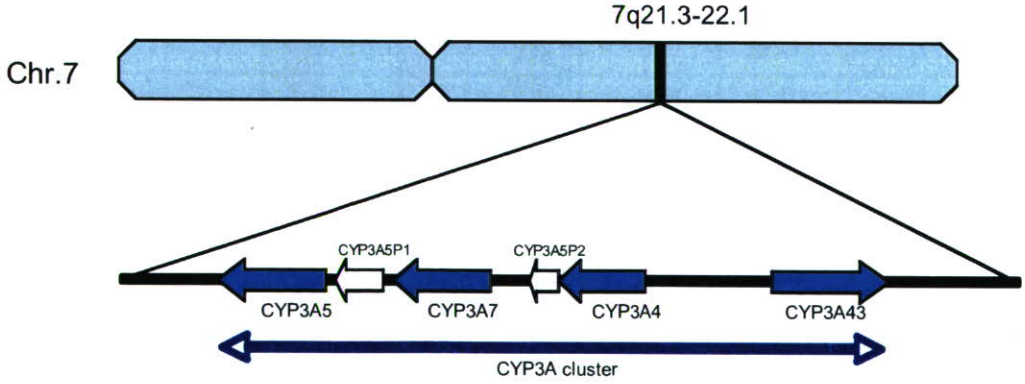

参考．miRNA の検索結果

## 参 Table 1. miRBase database search results for *CYP3A* and related nuclear receptor genes

| | miRNA | Score | Other candidate gene | Expression |
|---|---|---|---|---|
| CYP3A4 | hsa-miR-608 | 16.848 | 3A7 | Undetermined |
| | hsa-miR-372 | 16.598 | | O |
| | hsa-miR-302d | 16.598 | | Undetermined |
| | hsa-miR-330 | 16.593 | | O |
| | hsa-miR-206 | 16.469 | | O |
| | hsa-miR-27a | 16.446 | 3A43 | O |
| | hsa-miR-27b | 16.347 | 3A7, 3A43 | O |
| | hsa-miR-152 | 16.272 | 3A7 | O |
| | hsa-miR-578 | 16.174 | | Undetermined |
| | hsa-miR-216 | 16.149 | 3A43 | O |
| | hsa-miR-224 | 16.004 | 3A43 | O |
| CYP3A7 | hsa-miR-148a | 17.337 | PXR | O |
| CYP3A43 | hsa-miR-519a | 18.196 | | Undetermined |
| | hsa-miR-613 | 17.356 | 3A4, 3A7 | Undetermined |
| | hsa-miR-376a# | 17.161 | | O |

| | miRNA | Score | Other candidate gene | Expression |
|---|---|---|---|---|
| NR1I2 (PXR) | hsa-miR-522 | 16.823 | | Undetermined |
| | hsa-miR-594 | 16.591 | | O |
| | hsa-miR-597 | 16.212 | 3A43 | O |
| | hsa-miR-34a | 16.142 | | O |
| | hsa-miR-296 | Sloan-Kettering | | O |
| NR1I3 (CAR) | hsa-miR-432 | 18.160 | | O |
| | hsa-miR-565 | 17.912 | | O |
| | hsa-miR-571 | 17.718 | | Undetermined |
| | hsa-miR-503 | 17.709 | | O |
| | hsa-miR-618 | 17.376 | 3A43 | O |
| | hsa-miR-9 | 17.309 | 3A7, 3A5 | O |
| | hsa-miR-137 | 17.283 | 3A7 | O |
| | hsa-miR-338 | 16.404 | 3A7, 3A5 | O |

## 参 Fig. 3. miRBase database search result for *CYP3A4*

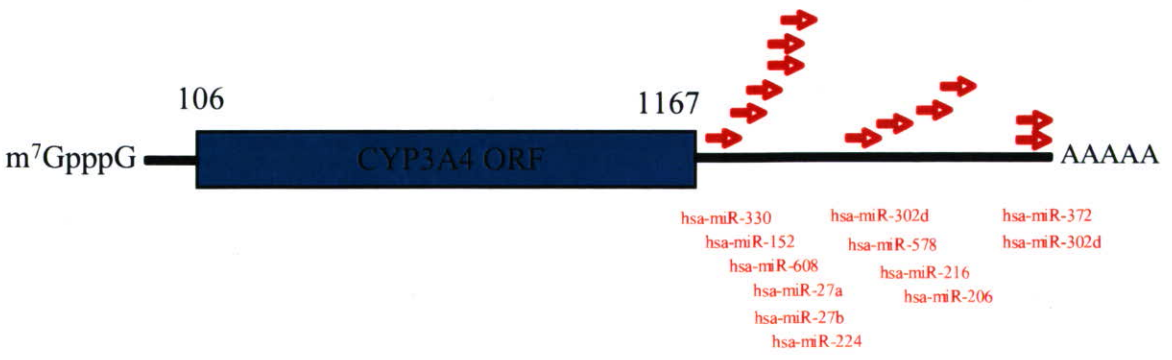

## Fig. 32. Correlation of *CYP3A* mRNA levels with related nuclear receptor gene levels in liver tissues

| CYP3A4 | CYP3A5 | CYP3A7 | CYP3A43 | PXR | CAR | RXRA | |
|---|---|---|---|---|---|---|---|
| | 0.2778 [ ] | 0.0036 [ ] | 0.6230 [**] | 0.6110 [**] | 0.5247 [**] | 0.4809 [**] | CYP3A4 |
| | | 0.4425 [*] | 0.1099 [ ] | 0.3021 [ ] | 0.1141 [ ] | 0.0856 [ ] | CYP3A5 |
| | | | 0.0775 [ ] | 0.0821 [ ] | -0.0991 [ ] | -0.1077 [ ] | CYP3A7 |
| | | | | 0.5816 [**] | 0.5468 [**] | 0.3767 [*] | CYP3A43 |
| | | | | | 0.6597 [**] | 0.5988 [**] | PXR |
| | | | | | | 0.8825 [**] | CAR |
| | | | | | | | RXRA |

r squared
p value ([**] : P< 0.01, [*] : P< 0.05)

## Fig. 33. The expression level of RNU48

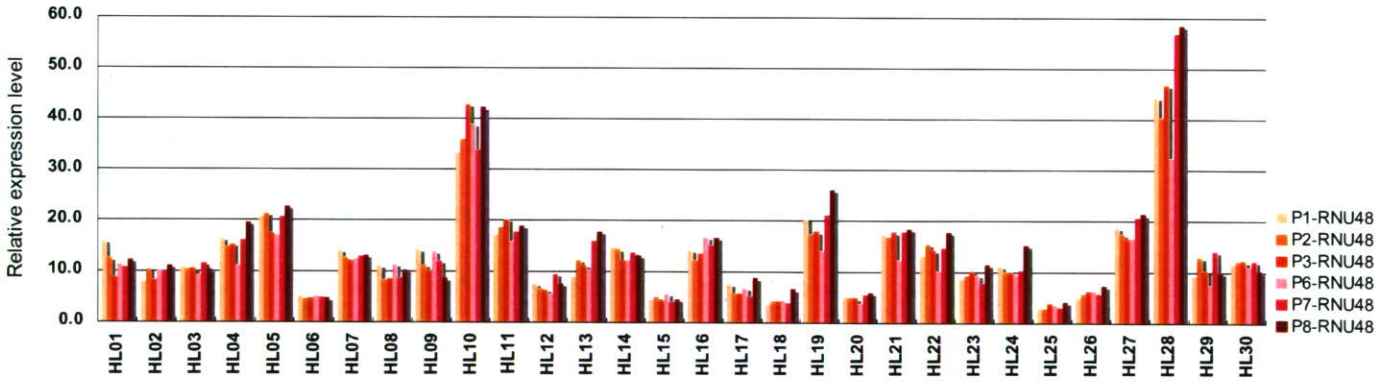


| | P1-RNU48 | P2-RNU48 | P3-RNU48 | P6-RNU48 | P7-RNU48 | P8-RNU48 |
|---|---|---|---|---|---|---|
| P1-RNU48 | 1.0000 | 0.9736 | 0.9601 | 0.9298 | 0.9635 | 0.9600 |
| P2-RNU48 | [**] | 1.0000 | 0.9819 | 0.9438 | 0.9623 | 0.9630 |
| P3-RNU48 | [**] | [**] | 1.0000 | 0.9534 | 0.9571 | 0.9698 |
| P6-RNU48 | [**] | [**] | [**] | 1.0000 | 0.8820 | 0.9051 |
| P7-RNU48 | [**] | [**] | [**] | [**] | 1.0000 | 0.9763 |
| P8-RNU48 | [**] | [**] | [**] | [**] | [**] | 1.0000 |

( r squared )

(p value [**]: P<0.01 )

## Fig. 34. The expression level of RNU44

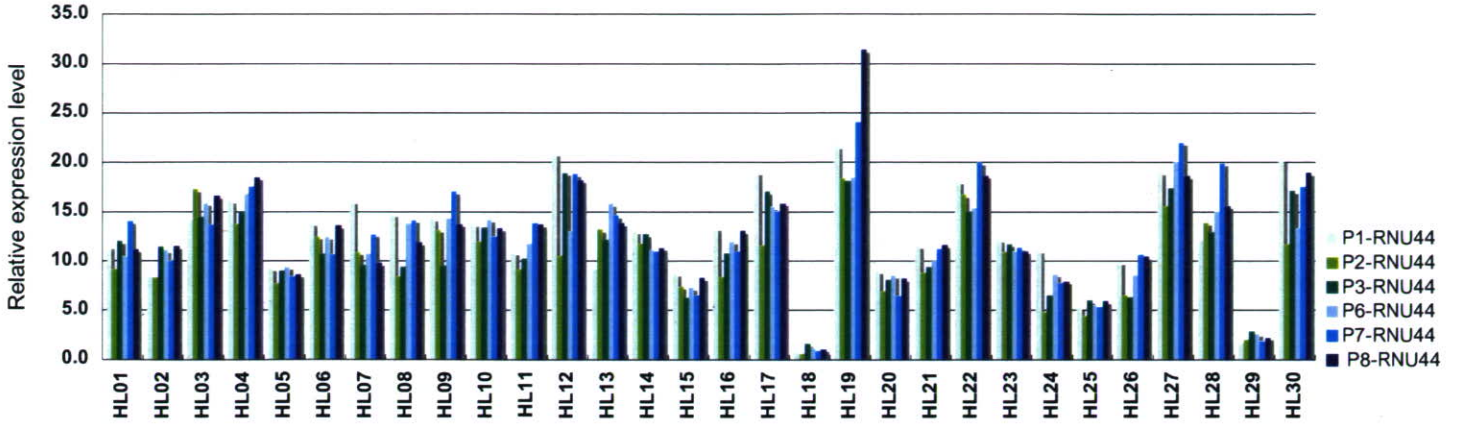


| | P1-RNU44 | P2-RNU44 | P3-RNU44 | P6-RNU44 | P7-RNU44 | P8-RNU44 |
|---|---|---|---|---|---|---|
| P1-RNU44 | 1.0000 | 0.7850 | 0.8932 | 0.8294 | 0.8678 | 0.8643 |
| P2-RNU44 | [**] | 1.0000 | 0.8347 | 0.9205 | 0.8712 | 0.8713 |
| P3-RNU44 | [**] | [**] | 1.0000 | 0.8712 | 0.8726 | 0.8827 |
| P6-RNU44 | [**] | [**] | [**] | 1.0000 | 0.9143 | 0.8768 |
| P7-RNU44 | [**] | [**] | [**] | [**] | 1.0000 | 0.9168 |
| P8-RNU44 | [**] | [**] | [**] | [**] | [**] | 1.0000 |

( r squared )

(p value [**]: P<0.01 )

## Fig. 35. The expression level of RNU6B

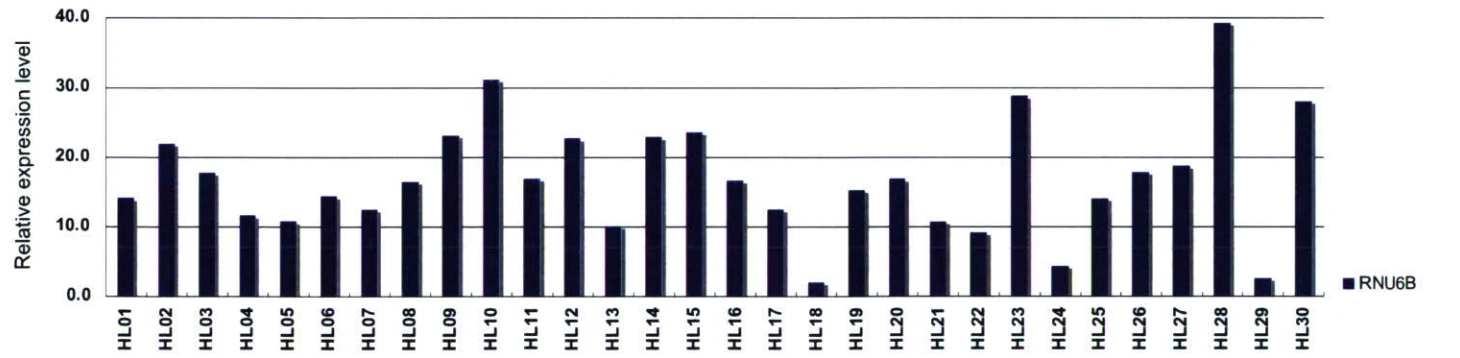


| | (P1-8) RNU48 | (P1-8) RNU44 | RNU6B |
|---|---|---|---|
| (P1-8) RNU48 | 1.0000 | 0.3615 | 0.4965 |
| (P1-8) RNU44 | [*] | 1.0000 | 0.3966 |
| RNU6B | [**] | [*] | 1.0000 |

( r squared )

( p value [**] : P< 0.01, [*] : P< 0.05)

## Fig. 36. Correlation of CYP3A mRNA expression levels with miRNA levels - normalized with RNU48 -

| | /RNU48 | CYP3A4 | CYP3A5 | CYP3A7 | CYP3A43 | PXR | CAR | RXRA |
|---|---|---|---|---|---|---|---|---|
| Pool-1 | miR-34a | -0.066 [ ] | -0.254 [ ] | 0.200 [ ] | -0.068 [ ] | -0.213 [ ] | -0.143 [ ] | -0.311 [ ] |
| | miR-372 | 0.394 [*] | -0.187 [ ] | -0.152 [ ] | 0.340 [ ] | 0.403 [*] | 0.229 [ ] | 0.163 [ ] |
| | miR-9 | 0.107 [ ] | -0.035 [ ] | 0.319 [ ] | 0.021 [ ] | -0.050 [ ] | -0.159 [ ] | -0.253 [ ] |
| | miR-137 | 0.114 [ ] | -0.033 [ ] | -0.096 [ ] | 0.219 [ ] | 0.407 [*] | 0.423 [*] | 0.554 [**] |
| Pool-2 | miR-27a | 0.185 [ ] | -0.226 [ ] | 0.120 [ ] | 0.093 [ ] | -0.034 [ ] | -0.104 [ ] | -0.205 [ ] |
| | miR-27b | 0.454 [*] | -0.100 [ ] | 0.001 [ ] | 0.353 [ ] | 0.076 [ ] | 0.146 [ ] | -0.021 [ ] |
| | miR-152 | 0.295 [ ] | -0.120 [ ] | 0.182 [ ] | 0.247 [ ] | 0.058 [ ] | 0.022 [ ] | -0.153 [ ] |
| | miR-296 | -0.233 [ ] | -0.212 [ ] | 0.108 [ ] | -0.267 [ ] | -0.307 [ ] | -0.257 [ ] | -0.378 [*] |
| Pool-3 | miR-148a | 0.379 [*] | 0.008 [ ] | -0.012 [ ] | 0.328 [ ] | 0.093 [ ] | 0.097 [ ] | -0.050 [ ] |
| | miR-206 | -0.192 [ ] | 0.088 [ ] | 0.076 [ ] | -0.266 [ ] | -0.034 [ ] | 0.149 [ ] | 0.307 [ ] |
| | miR-216 | 0.015 [ ] | 0.063 [ ] | 0.244 [ ] | -0.019 [ ] | -0.087 [ ] | 0.102 [ ] | 0.051 [ ] |
| | miR-330 | -0.042 [ ] | -0.219 [ ] | 0.115 [ ] | -0.138 [ ] | -0.260 [ ] | -0.232 [ ] | -0.359 [ ] |
| | miR-224 | -0.443 [*] | -0.345 [ ] | -0.002 [ ] | -0.412 [*] | -0.534 [**] | -0.354 [ ] | -0.487 [**] |
| | miR-432 | -0.015 [ ] | -0.395 [*] | -0.141 [ ] | -0.100 [ ] | -0.198 [ ] | -0.138 [ ] | -0.161 [ ] |
| Pool-6 | miR-338 | 0.079 [ ] | 0.053 [ ] | 0.526 [**] | 0.008 [ ] | 0.062 [ ] | -0.116 [ ] | -0.104 [ ] |
| | miR-503 | -0.202 [ ] | -0.341 [ ] | 0.172 [ ] | -0.169 [ ] | -0.217 [ ] | -0.345 [ ] | -0.366 [*] |
| Pool-7 | miR-376a | 0.098 [ ] | -0.331 [ ] | 0.006 [ ] | 0.076 [ ] | -0.079 [ ] | -0.152 [ ] | -0.201 [ ] |
| | miR-565 | 0.305 [ ] | 0.248 [ ] | 0.170 [ ] | 0.039 [ ] | 0.260 [ ] | -0.113 [ ] | 0.007 [ ] |
| | miR-594 | 0.333 [ ] | 0.003 [ ] | -0.099 [ ] | 0.069 [ ] | 0.266 [ ] | -0.045 [ ] | 0.000 [ ] |
| | miR-597 | 0.482 [**] | 0.010 [ ] | 0.258 [ ] | 0.379 [*] | 0.259 [ ] | 0.120 [ ] | 0.076 [ ] |
| Pool-8 | miR-618 | 0.268 [ ] | -0.098 [ ] | -0.102 [ ] | 0.020 [ ] | -0.003 [ ] | -0.033 [ ] | -0.118 [ ] |

r squared
p value ([**] : P< 0.01, [*] : P< 0.05)

Red column : (+) correlation, Blue column : ( - ) correlation

## Fig. 37. Correlation of CYP3A mRNA expression levels with miRNA levels - normalized with RNU44 -

| | /RNU44 | CYP3A4 | CYP3A5 | CYP3A7 | CYP3A43 | PXR | CAR | RXRA |
|---|---|---|---|---|---|---|---|---|
| Pool-1 | miR-34a | -0.309 [ ] | -0.327 [ ] | 0.027 [ ] | -0.214 [ ] | -0.140 [ ] | 0.265 [ ] | 0.201 [ ] |
| | miR-372 | 0.258 [ ] | -0.265 [ ] | -0.283 [ ] | 0.220 [ ] | 0.401 [*] | 0.283 [ ] | 0.265 [ ] |
| | miR-9 | -0.107 [ ] | -0.100 [ ] | 0.121 [ ] | -0.169 [ ] | -0.049 [ ] | -0.145 [ ] | -0.115 [ ] |
| | miR-137 | -0.071 [ ] | -0.013 [ ] | -0.069 [ ] | -0.124 [ ] | 0.161 [ ] | 0.453 [*] | 0.580 [**] |
| Pool-2 | miR-27a | -0.098 [ ] | -0.229 [ ] | -0.118 [ ] | -0.204 [ ] | 0.029 [ ] | 0.355 [ ] | 0.521 [**] |
| | miR-27b | 0.115 [ ] | -0.151 [ ] | -0.176 [ ] | 0.060 [ ] | 0.152 [ ] | 0.620 [**] | 0.726 [**] |
| | miR-152 | 0.011 [ ] | -0.162 [ ] | -0.010 [ ] | -0.011 [ ] | 0.122 [ ] | 0.500 [**] | 0.571 [**] |
| | miR-296 | -0.421 [*] | -0.215 [ ] | -0.045 [ ] | -0.505 [**] | -0.235 [ ] | 0.073 [ ] | 0.151 [ ] |
| Pool-3 | miR-148a | 0.299 [ ] | 0.109 [ ] | -0.068 [ ] | 0.453 [*] | 0.262 [ ] | 0.224 [ ] | 0.167 [ ] |
| | miR-206 | -0.101 [ ] | -0.013 [ ] | -0.059 [ ] | -0.169 [ ] | 0.053 [ ] | 0.250 [ ] | 0.380 [*] |
| | miR-216 | -0.061 [ ] | -0.018 [ ] | 0.116 [ ] | -0.043 [ ] | 0.040 [ ] | 0.522 [**] | 0.579 [**] |
| | miR-330 | -0.456 [*] | -0.083 [ ] | 0.324 [ ] | -0.415 [*] | -0.398 [*] | -0.426 [*] | -0.546 [**] |
| | miR-224 | -0.489 [**] | -0.297 [ ] | 0.075 [ ] | -0.414 [*] | -0.545 [**] | -0.348 [ ] | -0.515 [**] |
| | miR-432 | -0.214 [ ] | -0.355 [ ] | -0.221 [ ] | -0.235 [ ] | -0.049 [ ] | 0.070 [ ] | 0.262 [ ] |
| Pool-6 | miR-338 | 0.018 [ ] | 0.016 [ ] | 0.359 [ ] | -0.083 [ ] | 0.084 [ ] | 0.260 [ ] | 0.348 [ ] |
| | miR-503 | -0.435 [*] | -0.276 [ ] | 0.085 [ ] | -0.356 [ ] | -0.298 [ ] | -0.415 [*] | -0.371 [*] |
| Pool-7 | miR-376a | -0.146 [ ] | -0.342 [ ] | -0.083 [ ] | -0.146 [ ] | -0.077 [ ] | -0.092 [ ] | -0.017 [ ] |
| | miR-565 | 0.058 [ ] | 0.220 [ ] | 0.044 [ ] | -0.167 [ ] | 0.100 [ ] | -0.210 [ ] | -0.012 [ ] |
| | miR-594 | 0.064 [ ] | -0.010 [ ] | -0.118 [ ] | -0.110 [ ] | 0.114 [ ] | -0.152 [ ] | -0.036 [ ] |
| | miR-597 | 0.202 [ ] | 0.097 [ ] | 0.256 [ ] | 0.204 [ ] | 0.357 [ ] | 0.533 [**] | 0.670 [**] |
| Pool-8 | miR-618 | 0.193 [ ] | -0.124 [ ] | -0.301 [ ] | -0.080 [ ] | 0.154 [ ] | -0.114 [ ] | -0.147 [ ] |

r squared
p value ([**] : P< 0.01, [*] : P< 0.05)

Red column : (+) correlation, Blue column : ( - ) correlation

## Fig. 38. Correlation of CYP3A mRNA expression levels with miRNA levels - normalized with RNU6B -

| | /RNU6B | CYP3A4 | CYP3A5 | CYP3A7 | CYP3A43 | PXR | CAR | RXRA |
|---|---|---|---|---|---|---|---|---|
| Pool-1 | miR-34a | -0.266 [ ] | -0.344 [ ] | -0.093 [ ] | -0.274 [ ] | -0.331 [ ] | -0.133 [ ] | -0.225 [ ] |
| | miR-372 | 0.183 [ ] | -0.385 [*] | -0.353 [ ] | -0.010 [ ] | 0.116 [ ] | 0.002 [ ] | 0.060 [ ] |
| | miR-9 | -0.149 [ ] | -0.214 [ ] | 0.020 [ ] | -0.271 [ ] | -0.281 [ ] | -0.335 [ ] | -0.293 [ ] |
| | miR-137 | -0.218 [ ] | -0.097 [ ] | -0.241 [ ] | -0.259 [ ] | -0.044 [ ] | 0.107 [ ] | 0.273 [ ] |
| Pool-2 | miR-27a | -0.312 [ ] | -0.326 [ ] | -0.259 [ ] | -0.430 [*] | -0.320 [ ] | -0.202 [ ] | -0.145 [ ] |
| | miR-27b | -0.058 [ ] | -0.292 [ ] | -0.327 [ ] | -0.201 [ ] | -0.175 [ ] | 0.092 [ ] | 0.145 [ ] |
| | miR-152 | -0.243 [ ] | -0.287 [ ] | -0.220 [ ] | -0.344 [ ] | -0.282 [ ] | -0.129 [ ] | -0.141 [ ] |
| | miR-296 | -0.593 [**] | -0.378 [*] | -0.216 [ ] | -0.661 [**] | -0.537 [**] | -0.347 [ ] | -0.338 [ ] |
| Pool-3 | miR-148a | 0.011 [ ] | -0.254 [ ] | -0.353 [ ] | -0.073 [ ] | -0.130 [ ] | -0.036 [ ] | 0.005 [ ] |
| | miR-206 | -0.138 [ ] | -0.118 [ ] | -0.152 [ ] | -0.188 [ ] | -0.013 [ ] | 0.122 [ ] | 0.242 [ ] |
| | miR-216 | -0.110 [ ] | -0.250 [ ] | -0.042 [ ] | -0.138 [ ] | -0.055 [ ] | 0.488 [**] | 0.570 [**] |
| | miR-330 | -0.408 [*] | -0.338 [ ] | -0.168 [ ] | -0.489 [**] | -0.473 [**] | -0.349 [ ] | -0.387 [*] |
| | miR-224 | -0.495 [**] | -0.356 [ ] | -0.041 [ ] | -0.451 [*] | -0.544 [**] | -0.329 [ ] | -0.476 [**] |
| | miR-432 | -0.327 [ ] | -0.400 [*] | -0.371 [*] | -0.426 [*] | -0.271 [ ] | -0.103 [ ] | 0.032 [ ] |
| Pool-6 | miR-338 | -0.180 [ ] | -0.240 [ ] | 0.045 [ ] | -0.301 [ ] | -0.256 [ ] | -0.054 [ ] | 0.024 [ ] |
| | miR-503 | -0.473 [**] | -0.377 [*] | -0.209 [ ] | -0.507 [**] | -0.414 [*] | -0.443 [*] | -0.415 [*] |
| Pool-7 | miR-376a | -0.210 [ ] | -0.352 [ ] | -0.228 [ ] | -0.364 [*] | -0.199 [ ] | -0.224 [ ] | -0.193 [ ] |
| | miR-565 | -0.061 [ ] | 0.008 [ ] | -0.175 [ ] | -0.242 [ ] | -0.054 [ ] | -0.258 [ ] | -0.074 [ ] |
| | miR-594 | -0.021 [ ] | -0.113 [ ] | -0.195 [ ] | -0.174 [ ] | 0.009 [ ] | -0.198 [ ] | -0.079 [ ] |
| | miR-597 | 0.034 [ ] | -0.094 [ ] | -0.099 [ ] | -0.087 [ ] | -0.001 [ ] | 0.099 [ ] | 0.222 [ ] |
| Pool-8 | miR-618 | 0.081 [ ] | -0.229 [ ] | -0.257 [ ] | -0.175 [ ] | -0.024 [ ] | -0.118 [ ] | -0.126 [ ] |

r squared
p value ([**] : P< 0.01, [*] : P< 0.05)

Red column : (+) correlation, Blue column : ( - ) correlation

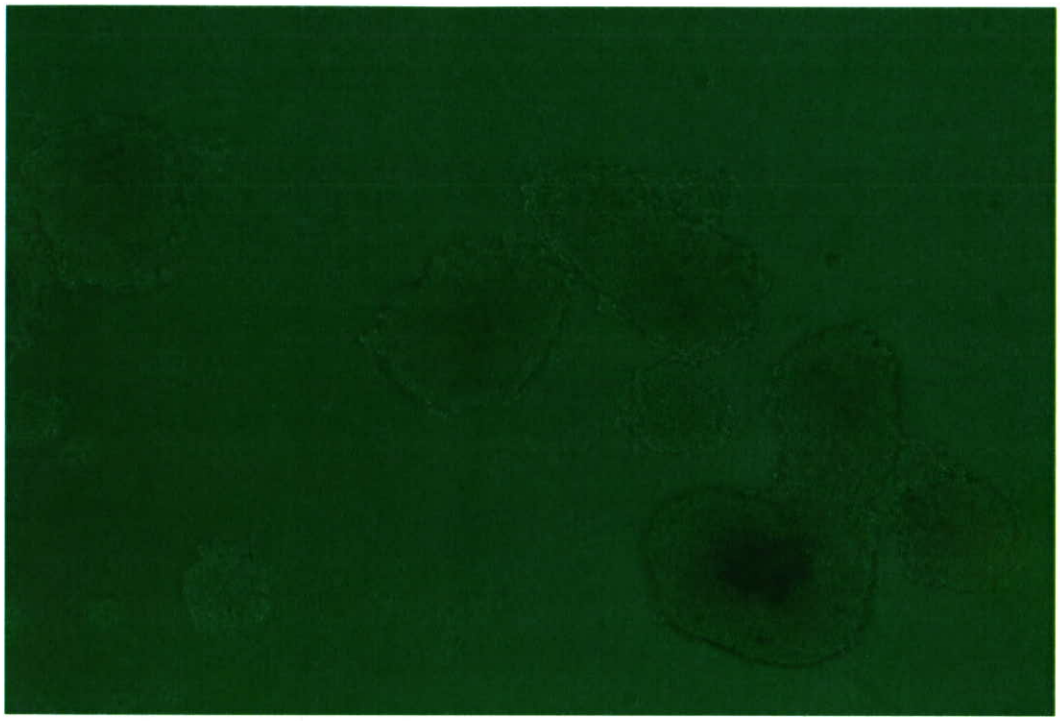

Fig. 39. SCIVAX 社ナノカルチャープレート NCP-L により、HepG2 細胞を 37℃、９６時間培養後に形成されたスフェロイドの位相差顕微鏡写真 (X100)。

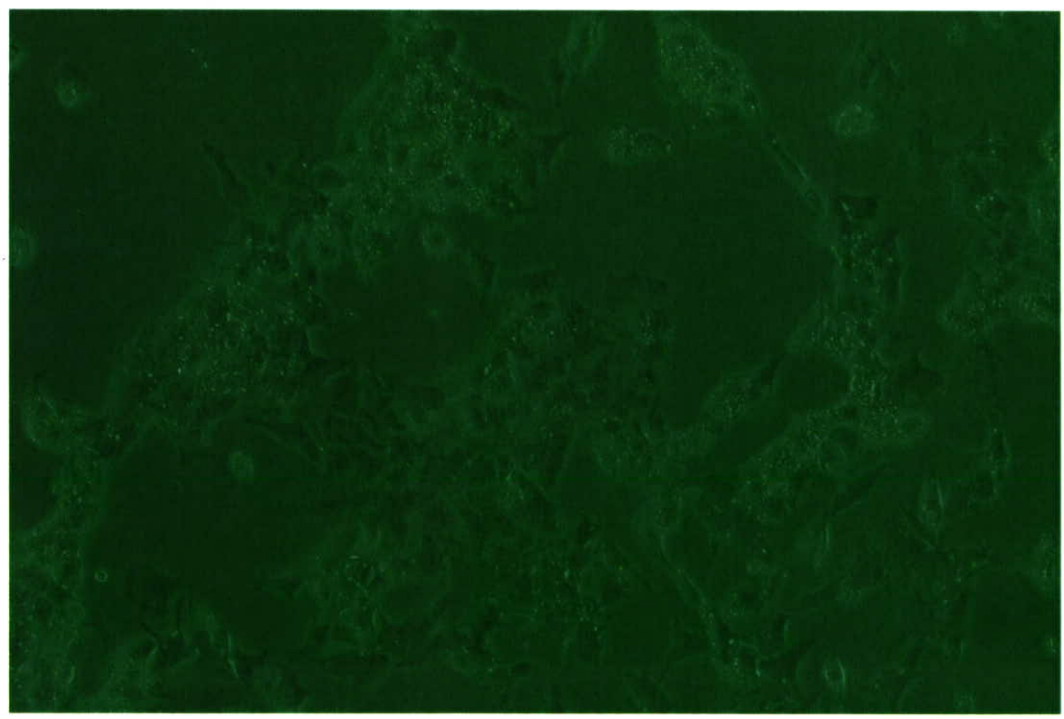

Fig. 40. Corning 社プラスチックプレートにより、HepG2 細胞を 37℃、９６時間平面培養後の細胞の位相差顕微鏡写真（X100)。

研究成果の刊行に関する一覧表

書籍

| 著者氏名 | 論文タイトル名 | 書籍全体の編集者名 | 書　籍　名 | 出版社名 | 出版地 | 出版年 | ページ |
|---|---|---|---|---|---|---|---|
| | | | | | | | |
| | | | | | | | |
| | | | | | | | |

雑誌

| 発表者氏名 | 論文タイトル名 | 発表誌名 | 巻号 | ページ | 出版年 |
|---|---|---|---|---|---|
| T. Hongo, M. Kajikawa, S. Ishida, S. Ozawa, Y. Ohno, J. Sawada, Y. Ishikawa and H. Honda | Gene expression property of high density three-dimensional tissue of HepG2 formed in radial-flow bioreactor. | J. Biosci. Bioeng. | 101(3) | 243-250 | 2006 |
| | | | | | |
| | | | | | |

JOURNAL OF BIOSCIENCE AND BIOENGINEERING
Vol. 101, No. 3, 243–250. 2006
DOI: 10.1263/jbb.101.243



# Gene Expression Property of High-Density Three-Dimensional Tissue of HepG2 Cells Formed in Radial-Flow Bioreactor

Tomokatsu Hongo,[1,4] Mariko Kajikawa,[1] Seiichi Ishida,[2] Shogo Ozawa,[2] Yasuo Ohno,[2] Jun-ichi Sawada,[3] Yoichi Ishikawa,[1] and Hiroyuki Honda[4]*

*ABLE Corporation, 4-15 Higashigoken-cho, Shinjyuku-ku, Tokyo 162-0813, Japan,[1] Division of Pharmacology, National Institute of Health Sciences, 1-18-1 Kamiyoga, Setagaya-ku, Tokyo 158-8501, Japan,[2] Division of Biochemistry and Immunochemistry, National Institute of Health Sciences, 1-18-1 Kamiyoga, Setagaya-ku, Tokyo 158-8501, Japan,[3] and Department of Biotechnology, School of Engineering, Nagoya University, Furo-cho, Chikusa-ku, Nagoya, Aichi 464-8603, Japan[4]*

Received 3 October 2005/Accepted 20 December 2005

**In our previous study, we examined three-dimensional culture using 5-ml radial-flow bioreactor (RFB) and showed that genes encoding cell cycle related proteins were suppressed in a stable phase. In this study, we analyzed the gene expression profiles of RFB-cultivated HepG2 cells and found that vascular endothelial growth factor (VEGF) production was strongly induced in the stable phase compared with the growth phase or static two-dimensional culture. When human umbilical vein endothelial cells (HUVECs) were grown under the conditioned medium of the stable phase, it was found that the formation of new blood vessels was induced in the angiogenesis model. DNA microarray analysis showed that the expression levels of both genes related to cell cycle arrest and which are known as tumor markers have increased in the stable phase. This result suggests that HepG2 cells in the stable phase maintain an active tumor phenotype. In addition, the expression of genes induced in the hypoxic condition was also induced in the stable phase. When the culture was carried out under a higher dissolved oxygen (DO) concentration, VEGF production did not decrease significantly and the new blood-vessel-forming ability of the conditioned medium was not suppressed. This suggests that the induction of VEGF production in a stable phase is not affected by DO during the tested level. These results suggest that the RFB cell culture system may be used to assess tumor progression mechanism under three-dimensional condition *in vitro*.**

[**Key words:** three-dimensional high-density cell culture, radial-flow bioreactor, DNA microarray]

Recently, many types of bioreactors for three-dimensional high-density cell culture have been developed since these bioreactors contribute to the construction of highly functional tissue-like structures. The cellular functions of the constructed structure were measured and compared with those of two-dimensional static culture and it has been reported that some cell functions were improved (1–6). However, whole gene profiles under three-dimensional high-density culture remain unclear and genetic evidence of the effectiveness of three-dimensional high-density culture remains unclarified. Although Vladimir *et al.* (7) showed the difference between static culture and three-dimensional culture using the rotary cell culture system, there was not any explicit feature on their listed genes.

In our previous study (8), we demonstrated that the hepatoblastoma cell line, HepG2, can be cultured in a radial-flow bioreactor (RFB) for more than two weeks. The glucose consumption was almost stable after day 10 and the time-lapse changes in lactic acid production, glutamine consumption, and ammonia production were almost the same as that of glucose. From the preliminary experiment using DNA microarray, it was found that the expressions of genes related to cell cycle were suppressed and cells remained in the G0/G1 phase at the stable phase. The diameter of aggregated cells in the RFB was more than 200 μm and maintained albumin production. This is important information regarding cancer progression. From their clinical experience handling cancer patients, Aguirre *et al.* (9) showed that some primary cancers and most metastatic lesions undergo a period of dormancy before progressive growth. For progressive growth, tumor angiogenesis must be induced (10). Tumor dormancy is defined as a state of angiogenic independent growth in which solid tumor growth does not often exceed 2 mm in diameter (11). In addition, tumor cells during tumor dormancy generally remain in the G0/G1 phase. Some induction mechanisms of G0/G1 arrest have been clarified. Aguirre *et al.* (9) showed that the decrease in the urokinase plasminogen activator receptor level in human carcinoma HEp3 cells induced a protracted state of tumor dormancy with G0/G1 arrest. This recent study revealed that oncogene inactivation in liver cancer resulted in the rapid loss of the

* Corresponding author. e-mail: honda@nubio.nagoya-u.ac.jp
phone: +81-(0)52-789-3215 fax: +81-(0)52-789-3214

expression of the tumor marker protein, alpha-fetoprotein (AFP), the increase in the expression of liver cell markers, cytokeratin 8 and carcinoembryonic antigen, and the induction of tumor dormancy (12). Considering these results, tumor dormancy may be defined as (i) three-dimensional cancer cell aggregation without neovascularization, (ii) G0/G1 arrest under a dormant condition, (iii) the induction of angiogenesis and (iv) the downregulation of some tumor marker proteins in a dormant condition. Among these definitions, we assumed that the first and second definitions were reflected in our previous study (8). Therefore, we hypothesized that the HepG2 cell growth in the RFB is similar to cancer growth in patients; hence, we used the RFB culture system as *in vitro* model of cancer progression.

To demonstrate our hypothesis, we first investigate in the present paper the difference in the gene expression level between the growth phase and the stable phase during the RFB cultivation of HepG2 cells. We show also identified genes with induced expression, such as insulin-like growth factor binding protein 3 (IGFBP-3) and vascular endothelial growth factor (VEGF). IGFBP-3 is a mediator of the growth suppressing signals of cells (13). Hence, VEGF is one of the most potent and specific angiogenic factors of tumor-induced angiogenesis (14, 15). The clinical importance of VEGF for tumor growth is supported by the fact that most tumors produce VEGF and the inhibition of VEGF-induced angiogenesis significantly inhibits tumor growth *in vivo* (16–18).

Next, we demonstrate that the conditioned medium of the stable phase during the RFB cultivation of HepG2 cells induced both the proliferation of human umbilical vein endothelial cells (HUVECs) and angiogenesis *in vitro*. Under a higher dissolved oxygen (DO) concentration during the RFB cultivation of HepG2 cells, the productivity of VEGF at the stable phase is suppressed incompletely. Compared with static culture condition, three-dimensional high-density culture in the RFB mimics normal physiological condition and our results indicate that the RFB culture of cancer cells will contribute greatly in clarifying the mechanism of the tumor growth progression *in vitro*.

## MATERIALS AND METHODS

**Culture of HepG2 cells** Hepatoblastoma cell line, HepG2, was obtained from American Type Culture Collection (Rockville, MD, USA). HepG2 cells were cultured in tissue culture dishes (59 $cm^2$; BD Biosciences, San Jose, CA, USA) and cell passaging was performed as described previously (8). Conditioned medium from static culture was collected from the culture dishes and stored at −80°C.

**Culture of HUVECs** Human umbilical vein endothelial cells (HUVECs) were obtained from Takara Bio (Kyoto). HUVECs ($1 \times 10^5$ cells) were cultured in tissue culture flask (25 $cm^2$; BD Biosciences) with 5 ml of EBM-2 (Takara Bio) at 37°C in an incubator containing 5% $CO_2$. Cell passasing was performed every 3 d with trypsin/EDTA (0.05% trypsin, 0.53 mM EDTA-4Na; Gibco/BRL, Gaithersburg, MD, USA), which was utilized to detach the cells.

**Culture in RFB** A 5 ml RFB (ABLE, Tokyo) and an RFB cell culture system shown in Fig. 1 were used in this study for the culture of HepG2 cells as described previously (8). Hydroxyl apatite (Pentax Corporation, Tokyo) with a diameter of 0.6–1.0 mm was used as a scaffold. The relatively large particle contributes in reducing the back pressure of the fixed bed and provides much space for cell growth. The particles were filled in the inner space of the RFB (Fig. 1B). Homogeneous flow was observed from a tracer experiment using dye. HepG2 cells at $3 \times 10^7$ were inoculated into the chamber medium and circulated between the chamber medium and the RFB at 7 ml/min. After 16 h from inoculation, there were no remaining cells in the chamber medium. The volume of the chamber medium was maintained at 200 ml and fresh medium was added continuously from the third day. The flow rate of the fresh medium was 250 ml/d. The DO concentration of the effluent of the RFB was controlled at 4.0 ppm. Under a higher DO concentration, the effluent DO concentration was controlled at 8.0 ppm. pH was controlled at 7.6 and the measured concentrations of glucose, lactic acid, glutamine and ammonia in the culture media were controlled by BF-4 (Oji Scientific Instrument, Amagasaki). The cell counts in the RFB were determined on the basis of glu-

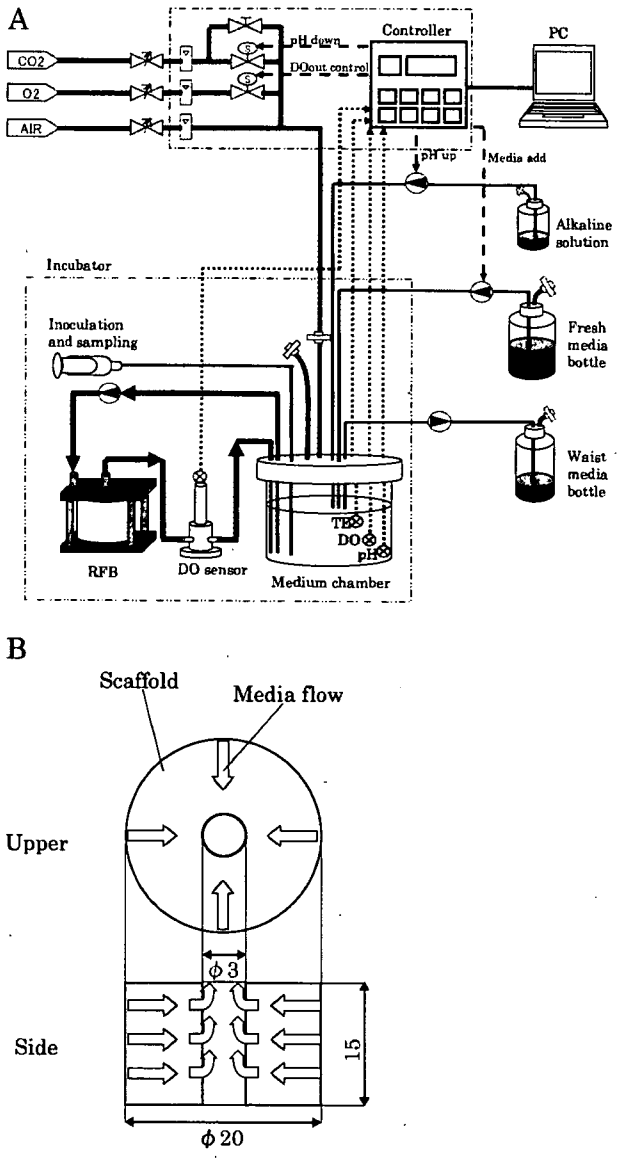


FIG. 1. Schematic of RFB cell culture system. (A) Culture system flow, (B) inner space of 5-ml RFB.

cose consumption rate. Conditioned medium was collected from the chamber medium at 7 d (growth phase) and 17 d (stable phase) and stored at −80°C. VEGF concentration in the medium was measured using the 96-wells-VEGF Human Assay kit (Amersham Biosciences UK limited, Buckinghamshire, UK).

**mRNA isolation and DNA microarray analysis** After culturing the HepG2 cells for 7 d and 17 d in the RFB, mRNA was isolated from the scaffold as described in previously paper (8). Samples were collected from three points in the RFB (peripheral, middle and central points). The conversion of total RNA (10 μg) to the target for Affymetrix GeneChip DNA microarray (Affymetrix, Santa Clara, CA, USA) hybridization was performed according to the manufacturer's instruction. DNA microarrays were scanned and obtained images were analyzed using the GeneChip Expression Analysis Software (ver. 5.0) (Affymetrix). DNA microarray analysis was performed in duplicate for each sample and the average signal intensities of 7 d and 17 d were calculated. The induced genes in the stable phase were identified on the basis of the following scheme described below: (i) genes whose expression levels on 17 d when divided by the data on 7 d yielded a value higher than 3, (ii) genes whose expression levels from a duplicate analysis were within 1.5-fold margin of increase, (iii) genes whose p-value was less than 0.01 when the t-test was performed on the microarray data from 7 d to 17 d. RFB culture was carried out twice for 7 d and 17 d. The four kinds of list of induced genes were compared and genes that were listed in all four kinds of list were selected.

**HUVEC proliferation assay** HUVECs ($1 \times 10^5$ cells) were inoculated in tissue culture flask (25 $cm^2$) containing 5 ml of EBM-2 and cultured for 24 h. After EBM-2 was removed, HUVECs were treated with 5 ml of the collected conditioned medium from the RFB culture for 48 h. Dulbecco's modified Eagle medium (DMEM; Gibco/BRL) was used for treating the negative control and EBM-2 was used for treating the positive control. After the cultivation under each condition, HUVECs were collected from the culture flasks and the number of cells was counted using a hemocytometer. The cell numbers of the HUVEC culture treated with the conditioned medium from the RFB culture or of the negative control were divided by the cell number of the positive control and the resulting ratio was defined as ratio to positive control. The VEGF concentration of the conditioned medium was measured as described above and the experiments were performed under the same levels of VEGF concentration.

**Blood vessel formation assay** Blood vessel formation assay was performed using an angiogenesis kit (Kurabo Industries, Osaka). Conditioned medium was diluted with the control medium supplied in the kit at 1:1. Diluted medium was added to the corresponding well and incubated according to the manufacturer's instruction. VEGF-A (Kurabo) was added to the control medium (final concentration: 10 ng/ml) and this medium was used as control. Newly formed blood vessels were stained by using the tubule staining kit (Kurabo) and observed by light microscopy. The length of blood vessels was analyzed by angiogenesis image analyzer (Kurabo). Angiogenesis ratio to control with 10 ng/ml was calculated by divided by the pixel obtained from control.

## RESULTS

**DNA mircoarray analysis** To clarify further the cell functions of HepG2 cells cultured in the RFB, we performed DNA microarray analysis with respect to cell samples from three points in the RFB. There were no significant differences between the three points (data not shown); thus the mean gene expression level from the three points was calculated and utilized in the analysis. Since HepG2 cells continuously grow forming multilayers even though the culture was already confluent, making it hard to achieve a stable growth condition of HepG2 2D culture because of confluency, we did not compare the gene expression profile of subconfluent HepG2 2D culture with that of confluent HepG2 2D culture. Then, the gene expression analysis of the stable phase was compared with that of the growth phase in 3D culture. As a result, 18 genes were selected as the genes induced in the stable phase. These selected genes are listed in Table 1. Okino *et al.* (19) reported that the expression of growth factor receptor-bound protein 10 (Grb10) mRNA in transformed primary cervical squamous cells was upregulated compared with noncancerous uterine squamous cells. Suganuma *et al.* (20) reported that angiotensin II receptor, type 1 (AT1R) was expressed in invasive ovarian adenocarcinomas. Except for these genes, six genes whose expression is common in cancer tissue exist (21–25). In addition, VEGF listed in Table 1 is known as a mitogen that specifically acts on endothelial cells and a major regulator for the induction of angiogenesis in tumors (14, 15).

On the other hand, insulin-like growth factor binding pro-

TABLE 1. Genes whose expressions were induced during stable phase

| Gene | Accession no. | Fold |
|---|---|---|
| Insulin-like growth factor binding protein 3 | BF340228 | 11.09 |
| Growth factor receptor-bound protein 10 | U66065 | 5.11 |
| Angiotensin II receptor, type 1 | NM_000685 | 4.65 |
| B cell RAG associated protein | NM_014863 | 3.97 |
| Apolipoprotein L, 1 | AF323540 | 3.89 |
| A kinase (PRKA) anchor protein (gravin) 12 | AB003476 | 3.83 |
| Sortilin-related receptor, L(DLR class) A repeats- containing | AV728268 | 3.64 |
| Vascular endothelial growth factor | AF022375 | 3.43 |
| Basic helix-loop-helix domain containing, class B, 2 | BG326045 | 3.41 |
| Adrenomedullin | NM_001124 | 3.34 |
| Family with sequence similarity 13, member A1 | NM_014883 | 3.34 |
| Solute carrier family 2 (facilitated glucose transporter), member 3 | NM_006931 | 3.32 |
| KIAA1199 protein | AB033025 | 3.28 |
| Lysyl oxidase | NM_002317 | 3.27 |
| Ribonuclease T2 | NM_003730 | 3.15 |
| Mitochondrial ribosomal protein S6 | AI867198 | 3.14 |
| Carbonic anhydrase IX | NM_001216 | 3.10 |
| Solute carrier organic anion transporter family, member 4A1 | NM_006342 | 3.00 |

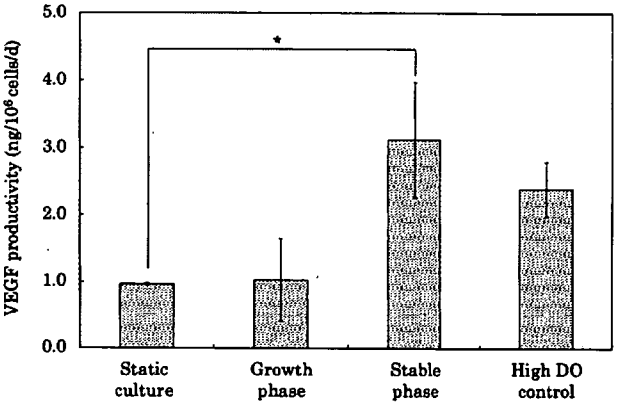


FIG. 2. VEGF productivity of HepG2 cells under static and 3D cultures in RFB. Static culture, culture in static culture flask; growth phase, culture in 5-ml RFB for 7 d; stable phase, culture 5-ml RFB for 17 d; high DO control, culture 5-ml RFB for 17 d below 8.0 ppm concentration. Asterisks indicate a significant difference between the static culture and stable phase (* $P<0.01$). Values are expressed as mean±SD for two independent cultures.

tein 3 (IGFBP-3) was also listed in Table 1. Treatment of hepatocellular carcinoma with IGFBP-3 led to a significant reduction in cell proliferation (26). In addition, A kinase anchor protein 12 and lysyl oxidase are known as tumor suppressor genes (27). In our previous report, cell cycle in the RFB cell culture system at the stable phase was arrested in most cells (8). Therefore, these results suggest that the stable phase of the RFB cultivation of HepG2 cells mimics the dormancy phase of tumor progression.

**Production of VEGF during RFB cultivation**

Whereas the above complex patterns of gene expression were demonstrated, there was a marked induction of VEGF expression which serves an important function in highly proliferating tumors. To demonstrate that HepG2 cells cultured in the RFB can release VEGF into the culture medium, we measured VEGF concentration and VEGF productivity was calculated. Figure 2 shows the VEGF productivity during the static culture, exponential growth phase and stable growth phase of the cell culture. VEGF productivity during the growth phase was almost the same as that during the static phase. However, VEGF productivity during the stable phase was approximately 3-fold higher than that of the static culture. The mean VEGF concentrations in the culture media were 51.5 pg/ml during the stable phase and 20.5 pg/ml during the growth phase. The calculated VEGF production rates were 1700 mg/d during the stable phase and 700 mg/d during the growth phase. Cell number was calculated on the basis of glucose consumption and the glucose consumption rates were $3.5\times10^{-3}$ mol/d during the stable phase and $2.9\times10^{-3}$ mol/d during the growth phase. Moreover, since the RFB culture was carried out by fed-batch operation, glucose (1.6–2.0 g/*l*) and glutamine concentrations in the culture media were not decreased and lactic acid and ammonia in the culture media were not excessively accumulated. Sone *et al.* (28) reported that VEGF production rate in bovine retinal pigmented epithelial cell culture was significantly increased by a decrease in glucose concentration from 5.5 to 0.5 mM, but not by a decrease in glucose

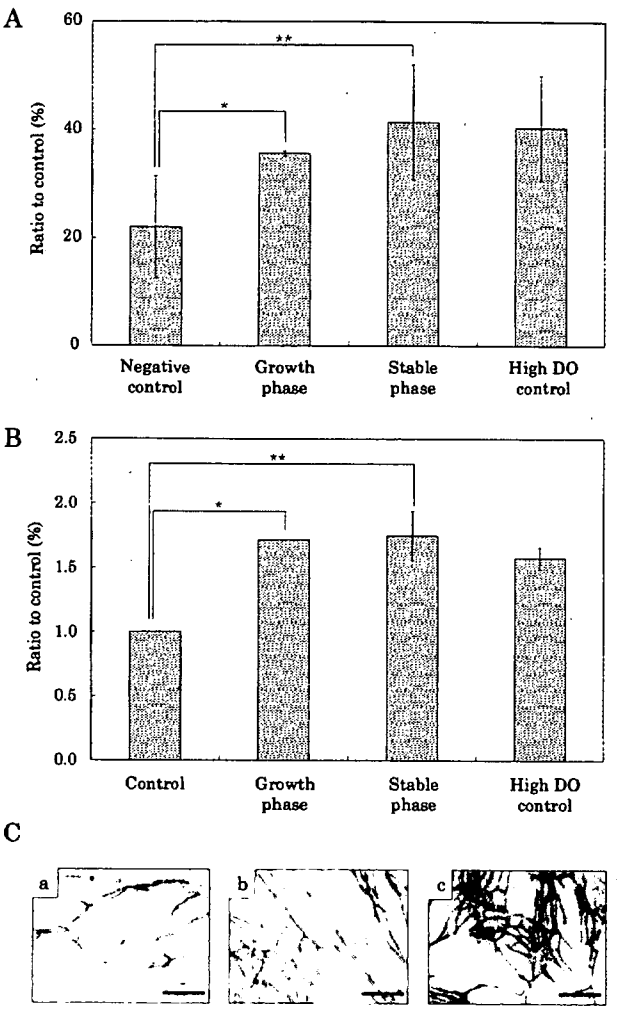


FIG. 3. Effects of conditioned medium on cultured HepG2 cells in 5-ml RFB. (A) HUVEC proliferation rate. The VEGF concentrations are 0 ng/ml (negative control), 4.8 ng/ml (growth phase), 4.6 ng/ml (stable phase), and 4.3 ng/ml (high DO control). The number of HUVECs cultured with the conditioned medium or in the negative control was divided by the number of cells in the positive control and the calculated ratio was defined as ratio to positive control. Asterisks indicate a significant difference (* $P<0.01$, ** $P<0.01$). Values are expressed as mean±SD for four independent cultures. (B) Angiogenesis assay. The VEGF concentrations are 10 ng/ml (control), 4.8 ng/ml (growth phase), 4.6 ng/ml (stable phase), and 4.3 ng/ml (high DO control). Ratio to control was calculated by divided by the pixel obtained from control. Asterisks indicate a significant difference (* $P<0.01$, ** $P<0.05$). Values are expressed as mean±SD for four independent cultures. (C) Light microscopic observations of newly formed blood vessels. a, Control; b, growth phase conditioned medium; c, stable phase conditioned medium. The bars represent 100 μm.

concentration from 16.5 to 5.5 mM. Therefore, we considered that the difference in VEGF productivity is not due to changes in the nutrient concentration in the culture media.

Next, HUVEC proliferation induced by the released VEGF in the conditioned medium of the RFB was also investigated. As shown in Fig. 3A, HUVEC proliferation was induced by the addition of the conditioned medium. When the same concentration of VEGF was used, the same proliferation rate was observed during the growth phase and the sta-

ble phase. Angiogenesis assay was also performed using the conditioned medium of the RFB. As shown in Fig. 3B and 3C, angiogenesis was observed and the ratio of blood vessel formation was almost the same between the growth phase and the stable phase when similar VEGF concentration was used. These results suggested that the released VEGF induced HUVEC proliferation and angiogenesis and the amount of VEGF produced during the growth phase and the stable phase were almost the same even though the production rate of VEGF was different between the growth phase and the stable phase.

We have confirmed that angiogenesis was strongly induced and the expressions of some tumor marker genes were suppressed during the stable phase. The essential features of tumor dormancy were described in the Introduction and our results match well with the described features. Therefore, we suggest that the stable phase of HepG2 cell culture in an RFB can be used as a tumor dormancy model, although some of genes were induced in the stable phase.

**Effect of higher DO concentration during RFB cultivation** Hermes *et al.* (29) showed that hypoxia showed the mRNA expression of the gene encoding erythropoietin and VEGF. VEGF expression was regulated by hypoxia-inducible factor-1(HIF-1) and the expression level of HIF-1 was increased in a hypoxic condition in HepG2 cell culture (30). To investigate the effects of DO on VEGF production rate in the RFB culture, we examined RFB cultivation at 8.0 ppm DO and measured VEGF concentration. VEGF productivity was lower than that at 4.0 ppm DO (Fig. 2), although it was still higher than those of the static culture and the growth phase. Below 8.0 ppm DO, the DO concentration of the inlet was approximately 16.0 ppm in the stable phase. This DO was 1.5-fold higher than that (10.0 ppm) below 4.0 ppm DO in the stable phase and we assumed that oxygen was sufficiently supplied to the cells in these two culture conditions in the RFB. Since there were no differences in glucose consumption rate, lactic acid production rate, glutamine consumption rate, and ammonia production rate between 4.0 ppm DO and 8.0 ppm DO, we considered that VEGF production was not affected under such high DO concentration. Moreover, HUVEC proliferation rate and blood vessel formation rate were almost the same (Fig. 3A, B). Platelet-derived growth factor (PDGF) and basic fibroblast growth factor (bFGF) are also known as angiogenesis inducing factors (31). We also measured the concentrations of PDGF and FGF in the conditioned medium of the RFB. However, PDGF and FGF were not detected (data not shown). Therefore, it was found that only the production of VEGF from HepG2 cells cultured in the RFB was strongly induced during the stable phase, whereas VEGF production was not regulated by DO concentration, and HUVEC proliferation rate and blood vessel formation rate were increased by the released VEGF. In the microarray analysis, the signal of HIF-1 was not induced in the stable phase compared with the growth phase and the static culture (data not shown). Mizukami *et al.* (32) showed that HIF-1 knockdown cells transplanted to mouse can induce angiogenesis and 50% the VEGF productivity of transplanted cells was maintained. This supported our results that the induction of VEGF during the stable phase of the RFB cultivation is not regulated by DO concentration. Therefore, RFB culture system may contribute to the construction of an *in vitro* model for angiogenesis or tumor progression and may provide an alternative method of tumor transplantation model to animals.

## DISCUSSION

In our previous study, we demonstrated that the cultivation of HepG2 cells in a 5-ml RFB showed a high function similar to normal liver cells in the human body (8). To clarify cellular function in more detail, we performed DNA microarray analysis. The induced genes are listed in Table 1 and there was 18. Among the genes induced, we found that genes encoding some tumor marker proteins were induced during the stable growth phase rather than genes encoding liver specific functional proteins. In particular, the expressions of Grb10 and ATR1 have already been demonstrated in tumorigenic tissues (19, 20). Excluding these genes, six of the 18 induced genes were ones which were induced in tumor tissue. VEGF is a mitogen that specifically acts on endothelial cells and is a major regulator for the induction of angiogenesis in tumors (14, 15). Therefore, the cultivation of HepG2 cells in the RFB can be used as a three-dimensional growth model of tumors. However, the expression of some tumor suppressor genes have also been shown to be induced during the stable phase of the cell cycle (26, 27). In addition, we demonstrated in our previous study that most HepG2 cells during the stable phase remained in the G0/G1 phase (8). Therefore, we suggest that the RFB cultivation of HepG2 cells can be used as a model of tumor dormancy of highly proliferating tumors. Aguirre *et al.* (9) showed that the suppression of ERK signaling by the downregulation of urokinase plasminogen activator receptor induced tumor dormancy with G0/G1 arrest. As shown in Table 1, the induction of the expressions of IGFBP-3 and Grb10 has been demonstrated. IGFBP-3 has the ability to block the binding of IGF to the IGF receptor (33). Grb10 is known as a negative regulator of Grb2 which is a stimulator of the ERK signaling pathway (34). Thus, these proteins are associated with the suppression of IGF-receptor-mediated signal transduction pathway; the activation of this pathway stimulates cell proliferation via ERK activation (35). Our results from the microarray analysis suggest that cell cycle arrests during RFB cultivation in the stable phase may be induced by ERK inactivation via IGF receptor downregulation or a similar suppression of tyrosine kinase-receptor-mediated signal transduction pathway. Clinical experience in cancer patients showed that some primary cancers and most highly-metastatic cancer cells undergo dormancy before entering the stage of progressive growth (9). The cultivation of HepG2 cells in the RFB did not induce angiogenesis. Therefore, the RFB cultivation of cancer cells can be used as an *in vitro* model of tumor dormancy which is clinically observed in cancer patients.

In this report, we also show that the VEGF productivity of HepG2 cells cultivated in the RFB during the stable phase was 3-fold higher than that during the growth phase and static culture. The conditioned medium from the stable phase and the growth phase induced HUVEC proliferation and an-

giogenesis (Fig. 3) *in vitro*. From these *in vitro* experiment, it is thought that HUVEC proliferation and migration were mediated exclusively via the kinase insert domain-containing receptor (KDR, also known as VEGF receptor-2) signaling pathway. On the other hand, fms-like tyrosine kinase 1 (flt-1, also known as VEGF receptor-1) activation mediated a distinctive inhibitory signaling pathway through PI-3K that downregulated cell proliferation pathway triggered by KDR (36). The induction of the expression of VEGF was stimulated by hypoxia (37), low glucose concentration (28, 38), cytokines (39), and estrogen (40). In particular, under a hypoxic condition, it has been shown that HIF-1 regulated the expression of VEGF and various hypoxia-induced proteins (41, 42). VEGF has mainly three isoforms (VEGF121, VEGF165, and VEGF189) as demonstrated by alternative splicing, and Herve *et al.* (43) have shown that VEGF165 and VEGF189 induced KDR but not flt-1 mRNA expression in HUVECs. Suzuki *et al.* (44) have shown that hypoxia-exposed HepG2 cells upregulated VEGF mRNA expression and VEGF release and hypoxia-exposed conditioned medium used for cultivating HepG2 cells induced flt-1 and KDR expressions in HUVECs. In the HUVEC proliferation and angiogenesis assays, we did not observe any significant differences between the cell cultures treated with the conditioned medium from the growth phase and from the stable phase when the assays were performed under almost the same VEGF concentration (Fig. 3). Therefore, these results suggest that the VEGF released from the RFB during the growth phase is a similar VEGF isoform to that released during the stable phase.

The expression of nine genes listed in Table 1 was induced by hypoxia in the static culture of HepG2 cells (45). However, during the RFB cultivation of HepG2 cells, the expression level of HIF-1 was not changed (data not shown). In addition, VEGF productivity under a high DO concentration did not change significantly (Fig. 2). Mizukami *et al.* (32) have shown that the hypoxic induction of VEGF expression was partially blocked in HIF-1 knock-down cancer cells; however, HIF-1 knock-down cancer cells which were tranfected to mouse maintained VEGF activity as shown by microvessel formation in xenografted cells. In addition, interleukin-8 (IL-8) expression was induced by hypoxia in HIF-1 knock-down cells via NF-kappaB activation. Bobrovniknva *et al.* (46) have shown that VEGF and IL-8 secretions were dramatically induced by glutamine deprivation in human breast carcinoma cells via NF-kappaB and activator protein-1 (AP-1) activations. Therefore, it is likely that the induction of VEGF expression in the RFB culture of HepG2 cells is induced by NF-kappaB activation. NF-kappaB could be activated by the exposure of cells to LPS or inflammatory cytokines such as TNF or interleukin-1, viral infection or viral gene products, UV irradiation, B or T cell activation, and by other physiological and nonphysiological stimuli (47). Further study is needed to clarify the mechanism of the induction of VEGF expression in the RFB cell culture system. In conclusion, the RFB cell culture system can be used to culture cancer cells with a dormant phenotype and is a useful device for clarifying the unknown mechanisms of the induction of angiogenic factors and the kinetics of tumor progression as an alternative method of tumor cell xenograft to laboratory animals.

## ACKNOWLEDGMENTS

We are deeply grateful to Ms. Serizawa and Mr. Wada of ABLE Corporation for assistance in the conduct of the RFB cell cultivation and the VEGF ELISA assay, and to Mr. Ino of Nagoya University for angiogenesis analysis. This study was supported by the Program for the Promotion of Fundamental Studies in Health Sciences and a grant (Research on Health Sciences Focusing on Drug Innovation) from the Japanese Health Sciences Foundation.

## REFERENCES

1. **Kawada, M., Nagamori, S., Aizaki, H., Fukaya, K., Niiya, M., Matsuura, T., Sujino, H., Hasumura, S., Yoshida, H., Mizutani, S., and Ikenaga, H.:** Massive culture of human liver cancel cells in a newly developed radial flow bioreactor system: ultrafine structure of functionally enhanced hepatocarcinoma cell lines. In Vitro Cell Dev. Biol. Anim., **34**, 109–115 (1998).
2. **Iwahori, T., Matsuura, T., Maehashi, H., Sugo, K., Saito, M., Hosokawa, M., Chiba, K., Masaki, T., Aizaki, H., Ohkawa, K., and Suzuki, T.:** CYP3A4 inducible model for *in vitro* analysis of human drug metabolism using a bioartificial liver. Hepatology, **37**, 665–673 (2003).
3. **Aizaki, H., Nagamori, S., Matsuda, M., Kawakami, H., Hashimoto, O., Ishiko, H., Kawada, M., Matsuura, T., Hasumura, S., Matsuura, Y., Suzuki, T., and Miyamura, T.:** Production and release of infectious hepatitis C virus from human liver cell culture in the three-dimensional radial-flow bioreactor. Virology, **314**, 16–25 (2003).
4. **Sakai, Y., Furukawa, K., and Suzuki, M.:** Immobilisation and long-term albumin secretion of hepatocyte spheroids rapidly formed by rotation tissue culture methods. Biotechnol. Tech., **6**, 527–532 (1992).
5. **Kurosawa, H., Yuminamochi, E., Yasuda, R., and Amano, Y.:** Morphology and albumin secretion of adalt rat hepatocytes cultured on a hydrophobic porous expanded polytetrafluoroethylene membrane. J. Biosci. Bioeng., **95**, 59–64 (2003).
6. **Yamada, K., Kamihira, M., and Iijima, S.:** Enhanced cell aggregation and liver functions using polymers modified with a cell-specific ligand in primary hepatocyte cultures. J. Biosci. Bioeng., **88**, 557–562 (1999).
7. **Khaoustov, V. I., Risin, D., Pellis, N. R., and Yoffe, B.:** Microarray analysis of genes differentiatially expression in HepG2 cell cultured in simulated microgravity: preliminary report. In Vitro Cell Dev. Biol. Anim., **37**, 84–88 (2001).
8. **Hongo, T., Kajikawa, M., Ishida, S., Ozawa, S., Ohno, Y., Sawada, J., Umezawa, A., Ishikawa, Y., Kobayashi, T., and Honda, H.:** Three-dimensional high-density culture of HepG2 cells in a 5-ml radial-flow bioreactor for construction of artificial liver. J. Biosci. Bioeng., **99**, 237–244 (2005).
9. **Aguiree Ghiso, J. A., Kovalski, K., and Ossowski, L.:** Tumor dormancy induced by downregulation of urokinase receptor in human carcinoma involves integrin and MAPK signaling. J. Cell Biol., **147**, 89–104 (1999).
10. **Folkman, J.:** Angiogenesis in cancer, vascular, rheumatoid and other disease. Nat. Med., **1**, 27–31 (1995).
11. **Mazure, N. M., Chen, E. Y., Laderoute, K. R., and Giaccia, A. J.:** Induction of vascular endothelial growth factor by hypoxia is modulated by a phosphatidylinositol 3-kinase/Akt signaling pathway in Ha-ras-transformed cells through a hypoxia inducible factor-1 transcriptional element. Blood, **90**, 3322–3331 (1997).
12. **Shachaf, C. M., Kopelman, A. M., Arvanitis, C., Karlsson, A., Beer, S., Mandl, S., Bachmann, M. H., Borowsky, A. D., Ruebner, B., Cardiff, R. D., Yang, Q., Bishop, J. M.,**

**Contag, C. H., and Felsher, D. W.:** MYC inactivation uncovers pluripotent differentiation and tumor dormancy in hepatocellular cancer. Nature, **431**, 1112–1117 (2004).

13. **Hanafusa, T., Yumoto, Y., Nouso, K., Nakatsukasa, H., Onishi, T., Fujikawa, T., Taniyama, M., Nakamura, S., Uemura, M., Takuma, Y., Yumoto, E., Higashi, T., and Tsuji, T.:** Reduced expression of insulin-like growth factor binding protein-3 and its promoter hypermethylation in human hepatocellular carcinoma. Cancer Lett., **176**, 149–158 (2002).
14. **Claffey, K. P. and Robinson, G. S.:** Regulation of VEGF/VPE expression in tumor cells: consequences for tumor growth and metastasis. Cancer Metastasis Rev., **15**, 165–176 (1996).
15. **Ferrara, N. and Alitalo, K.:** Clinical application of angiogenic growth factors and their inhibitors. Nat. Med., **5**, 1359–1364 (1999).
16. **Kim, K. J., Li, B., Winer, J., Armanini, M., Gillett, N., Phillips, H. S., and Ferrara, N.:** Inhibition of vascular endothelial growth factor-induced angiogenesis suppresses tumor growth *in vivo*. Nature, **362**, 841–844 (1993).
17. **Millauer, B., Shawver, L. K., Plate, K. H., Risau, W., and Ullrich, A.:** Glioblastoma growth inhibited *in vivo* by a dominant negative Flk-1 mutant. Nature, **367**, 576–579 (1994).
18. **Saleh, M., Stacker, S. A., and Wilks, A. F.:** Inhibition of growth of C6 glioma cells *in vivo* by expression of antisense vascular endothelial growth factor sequence. Cancer Res., **56**, 393–401 (1996).
19. **Okino, K., Konishi, H., Doi, D., Yoneyama, K., Ota, Y., Jin, E., Kawanami, O., and Takeshita, T.:** Up-regulation of growth factor receptor-bound protein 10 in cervical sequamous cell carcinoma. Oncol. Rep., **13**, 1069–1074 (2005).
20. **Suganuma, T., Ito, K., Shibata, K., Kajiyama, H., Nagasaka, T., Mizutani, S., and Kikkawa, F.:** Functional expression of the angiotensin II type 1 receptor in human ovarian carcinoma cells and its blockade therapy resulting in suppression of tumor invasion, angiogenesis, and peritoneal dissemination. Clin. Cancer Res., **11**, 2686–2694 (2005).
21. **Saarnio, J., Parkkila, S., Parkkila, A. K., Pastorekova, S., Haukipuro, K., Pastorek, J., Juvenen, T., and Kartunen, A. J.:** Transmembrane carbonic anhydrase, MN/CA IX, is a potential biomaker for biliary tumor. J. Hepatol., **35**, 643–649 (2001).
22. **Baer, S., Casaubon, L., Schwartz, M. R., Marcogliese, A., and Younes, M.:** Glut3 expression in biopsy specimens of laryngeal carcinoma is associated with poor survival. Laryngoscope, **112**, 393–396 (2002).
23. **Oehler, M. K., Fischer, D. C., Orlowska-Volk, M., Herrle, F., Kieback, D. G., Rees, M. C., and Bicknell, R.:** Tissue and plasma expression of the angiogenic peptide adrenomedullin in breast cancer. Br. J. Cancer, **89**, 1927–1933 (2003).
24. **Chakrabarti, L., Turley, H., Campo, L., Han, C., Harris, A. L., Gatter, K. C., and Fox, S. B.:** The transcription factor DEC1 (stra13, SHARP2) is associated with the hypoxic response and high tumor grade in human breast cancers. Br. J. Cancer, **91**, 954–958 (2004).
25. **Tang, Z. Y., Sun, F. X., Tian, J., Ye, S. L., Liu, Y. K., Liu, K. D., Xue, Q., Chen, J., Xia, J. L., Qin, L. X., and other 9 authors:** Metastatic human hepatocellular carcinoma models in nude mice and cell line with metastatic potential. World J. Gastroenterol., **7**, 597–601 (2001).
26. **Huynh, H., Chow, P. K., Ooi, L. L., and Soo, K. C.:** A possible role for insulin-like growth factor-binding protein-3 autocrine/paracrine loops in controlling hepatocellular carcinoma cell proliferation. Cell Growth Differ., **13**, 115–122 (2002).
27. **Lin, X., Nelson, P., and Gelman, I. H.:** SSeCKS, a major protein kinase C substrate with tumor suppressor activity, regulates G(1)→S progression by controlling the expression and cellular compartmentalization of cyclin D. Mol. Cell Biol., **20**, 7259–7272 (2000).
28. **Sone, H., Kawakami, Y., Okuda, Y., Kondo, S., Hanatani, M., Suzuki, H., and Yamashita, K.:** Vascular endothelial growth factor is induced by long-term high glucose concentration and up-regulated by acute glucose deprivation in cultured bovine pigmented epithelial cells. Biochem. Biophys. Res. Commun., **221**, 193–198 (1996).
29. **Hermes, M., Osswald, H., Mattar, J., and Kloor, D.:** Influence of an alter methylation potential on mRNA methylation and gene expression in HepG2 cells. Exp. Cell Res., **294**, 325–334 (2004).
30. **Hasebe, Y., Egawa, K., Yamazaki, Y., Kunimoto, S., Hirai, Y., Ide, Y., and Nose, K.:** Specific inhibition of hypoxia-inducible factor (HIF)-1 alpha activation and of vascular endothelial growth factor (VEGF) production by flavonoids. Biol. Pharm. Bull., **26**, 1379–1383 (2003).
31. **Jensen, R. L.:** Growth factor-mediated angiogenesis in the malignant progression of glial tumors: a review. Surg. Neurol., **49**, 189–195 (1998).
32. **Mizukami, Y., Jo, W. S., Duerr, E. M., Gala, M., Li, J., Zhang, X., Zimmer, M. A., Iliopoulos, O., Zukerberg, L. R., Kohgo, Y., Lynch, M. P., Rueda, B. R., and Chung, D. C.:** Induction of interleukin-8 preserves the angiogenic response in HIF-1alpha-dificient colon cancer cells. Nat. Med., **11**, 992–997 (2005).
33. **Payet, L. D., Wang, X. H., Baxter, R. C., and Firth, S. M.:** Amino- and carboxyl-terminal fragments of insulin-like growth factor (IGF) binding protein-3 cooperated to bind IGFs with high affinity and inhibit IGF receptor interactions. Endcrinology, **144**, 2797–2806 (2003).
34. **Dufresne, A. M. and Smith, R. J.:** The adaptor protein GRB10 is an endogeneous negative regulator of insulin-like growth factor signaling. Endocrinology, **146**, 4399–4409 (2005).
35. **Shiura, H., Miyoshi, N., Konishi, A., Wakisaka-Saito, N., Suzuki, R., Muguruma, K., Kohda, T., Wakana, S., Yokoyama, M., Ishino, F., and Kaneko-Ishino, T.:** Meg1/Grb10 overexpression causes postnatal growth retardation and insulin resistance via negative modulation of the IGF1R and IR cascade. Biochem. Biophys. Res. Commun., **329**, 909–916 (2005).
36. **Zeng, H., Dvorak, H. F., and Mukhopodyay, D.:** Vascular permeability factor (VPF)/vascular endothelial growth factor (VEGF) receptor-1 down-modulates VPF/VEGF receptor-2-mediated endothelial cell proliferation, but not migration, through phophatidylinositol 3-kinase-dependent pathway. J. Biol. Chem., **276**, 26969–26979 (2001).
37. **Wenger, R. H., Rolfs, A., Marti, H. H., Bauer, C., and Gassmann, M.:** Hypoxia, a novel inducer of acute phase gene expression in human hepatoma cell line. J. Biol. Chem., **270**, 27865–27870 (1995).
38. **Park, S. H., Kim, K. W., Lee, Y. S., Baek, J. H., Kim, M. S., Lee, Y. M., Lee, M. S., and Kim, Y. J.:** Hypoglycemia-induced VEGF expression is mediated by intercellular $Ca^{2+}$ and protein kinase C signaling pathway in HepG2 human hepatoblastoma cells. Int. J. Mol. Med., **7**, 91–96 (2001).
39. **Ren, Y., Cao, B., Law, S., Xie, Y., Lee, P. Y., Cheung, L., Chen, Y., Huang, X., Chan, H. M., Zhao, P., Luk, J., Vande Woude, G., and Wong, J.:** Hepatocyte growth factor promotes cancer cell migration and angiogenic factors expression: a prognostic marker of human esophageal squamous cell carcinomas. Clin. Cancer Res., **11**, 6170–6197 (2005).
40. **Mueller, M. D., Vigne, J. L., Minchenko, A., Lebovic, D. I., Leitman, D. C., and Taylor, R. N.:** Regulation of vascular endothelial growth factor (VEGF) gene transcription by estrogen receptors alpha and beta. Proc. Natl. Acad. Sci. USA, **97**, 10972–10977 (2000).
41. **Semenza, G. L.:** Regulation of mammalian O2 homeostasis by hypoxia-inducible factor 1. Annu. Rev. Cell Dev. Biol., **15**, 551–578 (1999).
42. **Semenza, G. L.:** HIF-1: mediator of physiological and patho-

physiological responses to hypoxia. J. Appl. Physiol., **88**, 1474–1480 (2000).
43. **Herve, M. A., Buteau-Lozano, H., Mourah, S., Calvo, F., and Perrot-Applanat, M.:** VEGF189 stimulates endpthelial cells proliferation and migration *in vitro* and up-regulates the expression of Flk-1/KDR mRNA. Exp. Cell Res., **309**, 24–31 (2005).
44. **Suzuki, H., Seto, K., Shinoda, Y., Mori, M., Ishimura, Y., Suematsu, M., and Ishii, H.:** Paracrine upregulation of VEGF receptor mRNA in endothelial cells by hypoxia-exposed Hep G2 cells. Am. J. Physiol., **276**, G92–97 (1999).
45. **Sonna, L. A., Cullivan, M. L., Sheldon, H. K., Pratt, R. E., and Lilly, C. M.:** Effect of hypoxia on gene expression by human hepatocytes (HepG2). Physiol. Genomics, **12**, 195–207 (2003).
46. **Bobrovnikova-Marjon, E. V., Marjon, P. L., Barbash, O., Vander Jagt, D. L., and Abcouwer, S. F.:** Expression of angiogenic factors vascular endothelial growth factor and interleukin-8/CXCL8 is highly responsive to ambient glutamine availability: role of nuclear factor-kappaB and activating protein-1. Cancer Res., **64**, 4858–4869 (2004).
47. **Baldwin, A. S., Jr.:** The NF-kappaB and I kappa B proteins: new discoveries and insights. Annu. Rev. Immunol., **14**, 649–683 (1996).